Inorganic Chemistry
Article
Cite This: Inorg. Chem. XXXX, XXX, XXX−XXX
pubs.acs.org/IC

Mechanistic Insight on the Formation of GaN:ZnO Solid Solution from Zn-Ga Layered Double Hydroxide Using Urea as the Nitriding Agent

Kiyofumi Katagiri,*[,†] Yuki Hayashi,[†] Risa Yoshiyuki,[†] Kei Inumaru,[†] Tomoki Uchiyama,[‡] Noriyuki Nagata,[‡] Yoshiharu Uchimoto,[‡] Akinobu Miyoshi,[¶] and Kazuhiko Maeda[¶]

[†]Department of Applied Chemistry, Graduate School of Engineering, Hiroshima University, 1-4-1 Kagamiyama, Higashi-Hiroshima, Hiroshima 739-8527, Japan

[‡]Graduate School of Human and Environmental Studies, Kyoto University, Yoshida Nihonmatsu-cho, Sakyo-ku, Kyoto 606-8501, Japan

[¶]Department of Chemistry, School of Science, Tokyo Institute of Technology, 2-12-1-NE-2 Ookayama, Meguro-ku, Tokyo 152-8550, Japan

Supporting Information

ABSTRACT: A solid solution of GaN and ZnO (GaN:ZnO) is promising as a photocatalyst for visible-light-driven overall water splitting to produce H_2. However, several obstacles still exist in the conventional preparation procedure of GaN:ZnO. For example, the atomic distributions of Zn and Ga are nonuniform in GaN:ZnO when a mixture of the metal oxides, i.e. Ga_2O_3 and ZnO, is used as a precursor. In addition, GaN:ZnO is generally prepared under a harmful NH_3 flow for long durations at high temperatures. Here, a facile synthesis of GaN:ZnO with homogeneous atomic composition via a simple and safe procedure is reported. A layered double hydroxide (LDH) containing Zn^{2+} and Ga^{3+} was used to increase the uniformity of the atomic distributions of Zn and Ga in GaN:ZnO. We employed urea as a nitriding agent instead of gaseous NH_3 to increase the safety of the reaction. Through the optimization of reaction conditions such as heat treatment temperature and content of urea, single-phase GaN:ZnO was successfully obtained. In addition, the nitridation mechanism using urea was investigated in detail. NH_3 released from the thermal decomposition of urea did not directly nitride the LDH precursor. X-ray absorption and infrared spectroscopies revealed that $Zn(CN_2)$-like intermediate species were generated at the middle temperature range and Ga−N bonds formed at high temperature along with dissociation of CO and CO_2.

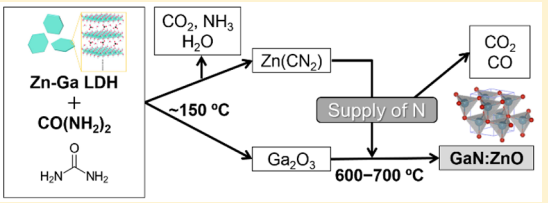

INTRODUCTION

Depletion of fossil fuels and related environmental issues have become a matter of serious concern for human society.[1−3] The search for clean and sustainable energy resources to address such issues is an important challenge for scientific communities. One of the most promising approaches to obtain a sustainable energy source is direct hydrogen (H_2) production via photocatalytic water splitting using semiconductor particles.[4−8] Although TiO_2 is an efficient photocatalyst, it can only work in the ultraviolet (UV) region because the band gap of TiO_2 is wider than 3 eV.[9] The sunlight that reaches the Earth's surface consists of nearly 45% visible light, 50% infrared (IR) radiation, and a smaller amount (only 4%) of UV radiation.[10] Therefore, great efforts have been devoted to developing novel photocatalysts that have overall water splitting capability under visible-light irradiation.[6−8,11,12] Chalcogenide materials, such as CdS, have a band edge potential suitable for water splitting under visible-light irradiation.[13] However, photocatalytic systems using such chalcogenides have not been successfully established because the instability of these materials limits oxygen production.[14,15]

Metal nitrides and oxynitrides are potential candidates for stable visible-light-driven photocatalysts for water splitting because the potential energy of N 2p orbitals is higher than that of O 2p orbitals.[12,16−19] In 2005, Maeda, Domen, and coworkers discovered that wurtzite gallium zinc oxynitride, a solid solution of GaN and ZnO (GaN:ZnO), can work as a photocatalyst to accomplish overall water splitting under visible-light irradiation.[20] Conventionally, GaN:ZnO is prepared by nitriding a mixture of metal oxides, i.e. Ga_2O_3 and ZnO, under an anhydrous NH_3 flow at high temperature (>800 °C).[20−24] However, this method is not favorable because of the risk associated with harmful NH_3 gas at high temperatures.[25,26] In addition, a relatively long reaction period is required to ensure that the two types of solid particles fuse to form a solid solution. Even after Ga_2O_3 and ZnO are nitrided for 15 h, the obtained GaN:ZnO has nonuniform atomic distributions of Zn and Ga.[24] Recently, Dukovic and coworkers reported the control of the elemental distribution in

Received: September 3, 2018

DOI: 10.1021/acs.inorgchem.8b02498
Inorg. Chem. XXXX, XXX, XXX−XXX

GaN:ZnO nanocrystals synthesized by the nitridation of a mixture of ZnO and $ZnGa_2O_4$ nanocrystals.[27,28] When the product was prepared at relatively low temperature, highly inhomogeneous GaN:ZnO particles with Ga and N enrichment near the surface and small aggregated particles with an ambiguous crystal structure were obtained. As the reaction temperature was raised (>800 °C), the elemental distribution of the product became increasingly more homogeneous. However, this approach still used high temperature and NH_3 gas to obtain GaN:ZnO with uniform Zn and Ga distributions.

In this study, we propose a facile method to prepare GaN:ZnO solid solutions that addresses the obstacles associated with their conventional preparation route. We use a layered double hydroxide (LDH) composed of Zn^{2+} and Ga^{3+} (hereafter denoted as Zn-Ga LDH) as a precursor of GaN:ZnO instead of a mixture of Ga_2O_3 and ZnO. Typically, LDHs are synthetic clay materials that can be denoted as $[(M^{2+})_{1-x}(M^{3+})_x(OH)_2]^{x+}(A^{n-})_{x/n}\cdot yH_2O$.[29−32] They contain brucite-like layers in which divalent cations (M^{2+}) are replaced by trivalent cations (M^{3+}), leading to a positively charged layered structure. The positive charges of the layers are compensated by the interlayer anions, such as CO_3^{2-}. Zn-Ga LDH can be synthesized by several solution processes, including coprecipitation, hydrothermal, and sol−gel methods.[33−37] Because Zn^{2+} and Ga^{3+} are homogeneously mixed in such solution-based processes, these ions are also homogeneously mixed on the atomic scale in the LDH brucite-like layers. Therefore, uniform distributions of Zn and Ga in GaN:ZnO can be obtained when Zn-Ga LDH is used as a precursor. Several groups have prepared GaN:ZnO with high Zn contents using Zn-Ga LDH as a starting material via relatively short heat treatment processes.[37−41] Chen and Skrabalak found that Zn volatilization during nitridation can be suppressed by maintaining a low partial pressure of O_2.[39] The suppression of Zn volatilization leads to materials with narrower band gaps and fewer structural defects. However, nitridation using gaseous NH_3 was still required to obtain GaN:ZnO even when Zn-Ga LDH was used as a precursor. Here, we use urea as a nitriding agent instead of gaseous NH_3. Urea is cheap, nontoxic, and noncorrosive and can be easily handled because it is in a solid state at ambient temperature.[42] Therefore, urea is used as a raw material in the manufacture of many chemicals, such as various plastics, urea−formaldehyde resins, and adhesives.[43] We consider it feasible to prepare GaN:ZnO using a conventional furnace. Several groups have reported the preparation of metal oxynitrides and nitrides using urea as a nitriding agent.[44−46] Rao and co-workers synthesized ternary metal oxynitrides with formulas of $MTaO_2N$ (M = Ca, Sr, Ba), $MNbO_2N$ (M = Sr, Ba), $LaTiO_2N$, and $SrMoO_{3-x}N_x$ by heating the corresponding metal carbonates and transition-metal oxides with excess urea.[44] Giordano et al. achieved the controlled synthesis of TaON and Ta_3N_5 using a method employing Ca^{2+} and urea.[46] However, the nitriding mechanism when urea is used is still not clear. Here, we optimize the transformation conditions from Zn-Ga LDH to GaN:ZnO, including heat treatment temperature and duration and mixing ratio of urea. The obtained samples are characterized by scanning electron microscopy (SEM), transmission electron microscopy (TEM), X-ray diffraction (XRD), UV−vis diffuse reflectance spectroscopy, and inductively coupled plasma−optical emission spectroscopy (ICP-OES). In addition, we investigate the nitridation mechanism of Zn-Ga LDH to obtain GaN:ZnO in the presence of urea as a nitriding agent. In particular, the X-ray absorption fine structure (XAFS) technique is used to resolve the local environments of Ga and Zn during the transformation of Zn-Ga LDH to GaN:ZnO. Both X-ray absorption near edge structure (XANES) and extended X-ray absorption fine structure (EXAFS) analyses are conducted, in combination with IR spectroscopy. Finally, we propose the nitridation mechanism when urea is used as a nitrogen source.

EXPERIMENTAL SECTION

Materials. Gallium(III) nitrate octahydrate ($Ga(NO_3)_3\cdot 8H_2O$; ≥99.0%), zinc(II) nitrate hexahydrate ($Zn(NO_3)_3\cdot 6H_2O$; ≥99.0%), gallium oxide (β-Ga_2O_3 (monoclinic, space group $A2/m$); 99.99%), zinc oxide (ZnO; 99.5%), urea (99%), sodium carbonate (Na_2CO_3; 99.8%), and sodium hydroxide (NaOH) solution (1 mol dm^{-3}) were purchased from Kishida Chemical Co., Ltd. (Osaka, Japan). Ethanol (≥99.5%) was obtained from Nacalai Tesque, Inc. (Kyoto, Japan). All reagents were used as received without further purification. The water used in all experiments was deionized with a Millipore Milli-Q system (Merck Millipore, Billerica, MA, USA).

Preparation of Zn-Ga LDH. Zn-Ga LDH was synthesized as reported previously.[37] Briefly, $Ga(NO_3)_3\cdot 8H_2O$ (5 mmol) and $Zn(NO_3)_3\cdot 6H_2O$ (10 mmol) were dissolved in deionized water and the metal ion concentration was adjusted to 0.15 mol dm^{-3}. The pH of the solution was adjusted to 8 by addition of an aqueous solution containing Na_2CO_3 (1.0 mol dm^{-3}) and NaOH (3.0 mol dm^{-3}). The mixture was incubated at 80 °C for 24 h to obtain a precipitate of Zn-Ga LDH. The precipitate was filtered and then washed several times with deionized water. Finally, the sample was dried overnight under vacuum.

Preparation of GaN:ZnO. Zn-Ga LDH was mixed with urea using an agate mortar and pestle. The mixture was heated at various temperatures (600−900 °C) under a N_2 flow (500 mL min^{-1}) using an alumina crucible boat in a horizontal tube furnace. The temperature of the furnace was raised to the final temperature over a fixed period of 3 h. The heating duration at the final temperature was varied from 2 to 24 h. For comparison, a mixture of Ga_2O_3 and ZnO ([Zn]/[Ga] = 2) was used a precursor instead of Zn-Ga LDH. In this case, [urea]/[Ga] was fixed to 3. The mixture of Ga_2O_3, ZnO, and urea was heated at 800 °C for 4 h under a N_2 flow (500 mL min^{-1}).

Characterization. Structural information about the samples was obtained by XRD (D8 Advance, Bruker AXS, Germany) using Cu Kα radiation. SEM images were captured with a Hitachi S-4800 microscope. TEM images were captured with a JEOL JEM-2010 microscope operating at 200 kV. Samples were prepared by depositing a droplet of each dispersion on carbon-coated copper grids covered with elastic carbon films and drying in air overnight. Molar ratios of Zn and Ga were determined using energy-dispersive X-ray (EDX) spectroscopy with a JED2300-T (JEOL) attached to the TEM. Ga and Zn contents were measured via ICP-OES using a Thermo Scientific iCAP 6500. UV−vis−near-infrared diffuse reflectance spectra were measured by a spectrophotometer (V-670, JASCO, Tokyo, Japan). The band gap (E_g) of the synthesized GaN:ZnO solid solution in this work was estimated using the conventional equation[4]

$$E_g\ (\mathrm{eV}) = 1240/\lambda\ (\mathrm{nm}) \quad (1)$$

where λ represents an absorption edge wavelength of the material. XAFS measurements were conducted on the BL01B1 beamline of the SPring-8 synchrotron facility (Hyogo, Japan) using a ring energy of 8 GeV to acquire Zn and Ga K-edge spectra. XAFS data were acquired at room temperature in transmission mode using a Si(111) double-crystal monochromator. A pair of Rh-coated mirrors was used to eliminate higher harmonics. XANES spectra were processed using the Athena software package.[47] Standard spectra of Ga_2O_3, ZnO, gallium nitride (GaN), zinc gallate ($ZnGa_2O_4$), and zinc cyanamide ($Zn(CN_2)$) were also collected. GaN was purchased from Mitsuwa Chemicals Co., Ltd., Japan. We synthesized $ZnGa_2O_4$ and $Zn(CN_2)$

DOI: 10.1021/acs.inorgchem.8b02498
Inorg. Chem. XXXX, XXX, XXX−XXX

(details are given in the Supporting Information). Fourier transform infrared (FT-IR) spectra were collected over the range of 2500−400 cm^{-1} with a JASCO FT/IR-4200 spectrometer fitted with a diffuse reflectance accessory. The gases released during the heat treatment process were analyzed using a quadrupole mass spectrometer (Q-MS). The mixture of Zn-Ga LDH and urea was heated under a flow of He gas.

RESULTS AND DISCUSSION

Optimization of Transformation Conditions from Zn-Ga LDH to GaN:ZnO. Initially, Zn-Ga LDH, which was used as a precursor of GaN:ZnO, was prepared by a typical solution process. Figure 1a shows an XRD pattern of the product that

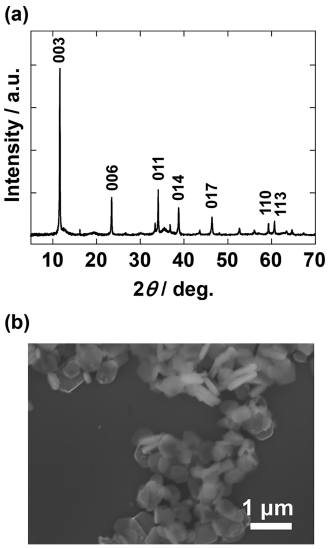

Figure 1. (a) XRD pattern and (b) SEM image of Zn-Ga LDH.

was prepared from the solution containing $Ga(NO_3)_3$ and $Zn(NO_3)_3$. All of the diffraction peaks can be attributed to a rhombohedral lattice with *R*3*m*, which is commonly used to describe LDH structures.[30] No peaks from impurities were discerned, indicating the high purity of the product. In addition, the diffraction peaks are sharp and symmetric, strongly suggesting that Zn-Ga LDH with relatively high crystallinity was obtained. The basal spacing corresponds to that of a CO_3^{2-}-containing LDH.[29] An SEM image of the Zn-Ga LDH sample is shown in Figure 1b. Similarly to previous reports,[33−35] the obtained Zn-Ga LDH crystallized into well-shaped hexagonal platelets with diameters of ca. 200−500 nm and a thickness of 50 nm. EDX analysis revealed that the [Zn]/[Ga] ratio of the sample was 2. Therefore, Zn-Ga LDH with an equal mixing ratio of cations to that of the raw materials was obtained.

Next, we examined the transformation of Zn-Ga LDH to GaN:ZnO using urea as a nitriding agent. After calcination of Zn-Ga LDH in the presence of urea, highly crystalline GaN:ZnO was obtained. Figure 2 shows optical photographs and XRD patterns of products obtained from mixtures of Zn-Ga LDH and urea with various mixing ratios after calcination. We used molar ratios of Ga in Zn-Ga LDH to urea ([urea]/[Ga] = *R*) of 2, 3, 4, 6, and 8. The calcination temperature and duration were fixed at 800 °C and 4 h, respectively. As depicted in Figure 2a, the mixture of Zn-Ga LDH and urea was white before calcination. After calcination, the products ranged from yellow (*R* = 6, 8) to brown (*R* = 2, 3, 4). These colored

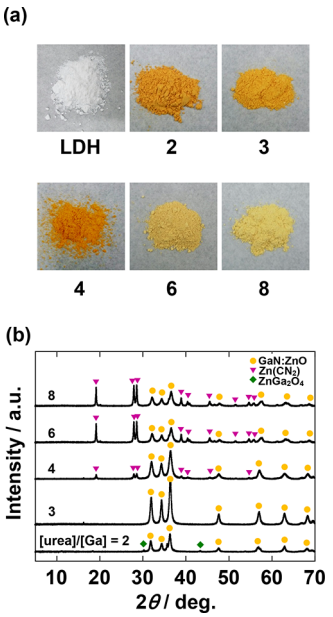

Figure 2. (a) Optical photographs and (b) XRD patterns of products obtained from mixtures of Zn-Ga LDH and urea with various mixing ratios (*R* = 2, 3, 4, 6, 8) after calcination at 800 °C for 4 h.

samples with visible light absorption clearly indicate that Zn-Ga LDH was transformed into GaN:ZnO. The XRD patterns in Figure 2b show that the obtained products consist of a single hexagonal wurtzite phase similar to that of GaN and ZnO. The peak positions lay between those of GaN and ZnO.[24] These results revealed that the obtained products were solid solutions of GaN and ZnO. In particular, the mixture with *R* = 3 gave a single phase of wurtzite structure without any other peaks. For the sample produced using *R* = 2, impurity peaks assignable to $ZnGa_2O_4$ spinel were found in addition to the peaks of GaN:ZnO. In contrast, the obtained product was a mixture of GaN:ZnO and $Zn(CN_2)$ when *R* > 4. The 101 diffraction peaks shifted to higher 2θ angles with increasing urea content (Figure S3). This indicates that the zinc concentration in the solid solution decreased because of the formation of $Zn(CN_2)$ as a byproduct. These results corresponded well to the yellowish color of the products obtained using a high ratio of urea. Therefore, the optimal mixing ratio to obtain GaN:ZnO without any impurities is *R* = 3; we used this ratio in subsequent experiments.

Figure 3 displays XRD patterns of products obtained from mixtures of Zn-Ga LDH and urea after calcination at various temperatures for 4 h. The calcination temperature was varied

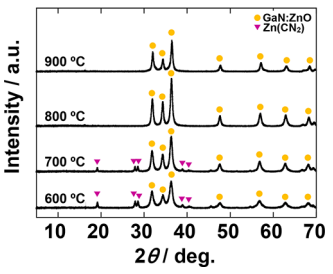

Figure 3. XRD patterns of products obtained from mixtures of Zn-Ga LDH and urea after calcination at various temperatures (600, 700, 800, and 900 °C) for 4 h.

DOI: 10.1021/acs.inorgchem.8b02498
Inorg. Chem. XXXX, XXX, XXX−XXX

from 600 to 900 °C. Reactions performed at all calcination temperatures resulted in products that could be indexed to a wurtzite phase of GaN:ZnO. When the calcination was carried out at 600 and 700 °C, $Zn(CN_2)$ formed as a byproduct. Therefore, a calcination temperature higher than 800 °C should be used to obtain single-phase GaN:ZnO. The 101 diffraction peak of the product obtained at 900 °C appeared at a 2θ angle higher than that of the material obtained at 800 °C (Figure S4). In addition, the product obtained at 900 °C was yellow, whereas that obtained at 800 °C was brown (Figure S5). These results indicate that the zinc concentration of the solid solution decreased by volatilization of the zinc component during calcination at high temperature. The observed peak shift is reasonable because the ionic radius of Zn^{2+} (0.74 Å) is larger than that of Ga^{3+} (0.61 Å).[48]

The influence of calcination duration on the transformation of Zn-Ga LDH to GaN:ZnO was also investigated. Figure 4

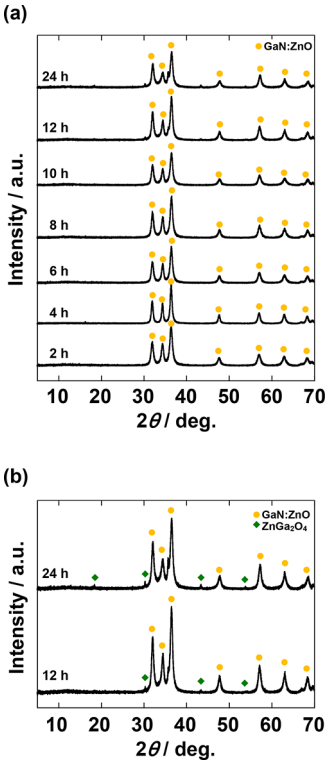

Figure 4. (a) XRD patterns of products obtained from mixtures of Zn-Ga LDH and urea after calcination at 800 °C for various periods (2–24 h). (b) Magnified patterns of products obtained by calcination for 12 and 24 h.

presents XRD patterns of products obtained from mixtures of Zn-Ga LDH and urea after calcination at 800 °C for various periods (2–24 h). As shown in Figure 4a, the wurtzite hexagonal structure of GaN:ZnO without any impurity phases was obtained after calcination for 2 h. When the calcination period was longer than 12 h, peaks assignable to $ZnGa_2O_4$ spinel appeared (Figure 4b). The 101 diffraction peaks shifted to higher 2θ angles with lengthening calcination period (Figure S6a). The zinc concentration of GaN:ZnO was decreased by volatilization of the zinc component during long periods of calcination. The products changed from brown to yellow as the calcination period lengthened (Figure S6b). This also supports volatilization of the zinc component during calcination. However, the shift of the 101 diffraction peak was suppressed after 10 h (Figure S6a). Therefore, these results indicate that calcination for long periods induced not only volatilization of the zinc component but also decomposition of GaN:ZnO to $ZnGa_2O_4$. For comparison, we tried to prepare GaN:ZnO using a mixture of Ga_2O_3 and ZnO instead of Zn-Ga LDH. An XRD pattern of the product obtained from the mixture of Ga_2O_3, ZnO, and urea (Ga:Zn:urea molar ratio 1:1:3) after calcination at 800 °C for 4 h is displayed in Figure S7. Peaks that indexed to not only GaN:ZnO but also $ZnGa_2O_4$ and $Zn(CN_2)$ were observed. Therefore, use of Zn-Ga LDH is essential to obtain single-phase GaN:ZnO when urea is used as a nitriding agent.

Characterization of GaN:ZnO Prepared from Zn-Ga LDH and Urea. Figure 5a shows a TEM image of GaN:ZnO

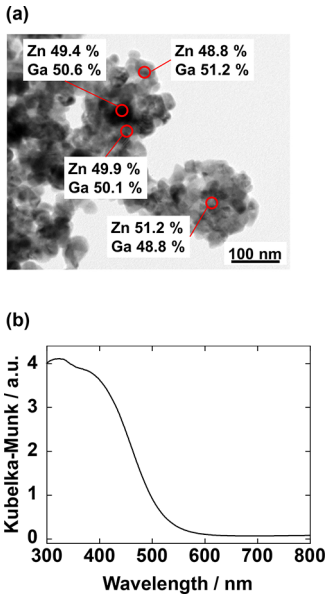

Figure 5. (a) TEM image and (b) UV–vis diffuse reflection spectrum of GaN:ZnO prepared from Zn-Ga LDH and urea (R = 3) by calcination at 800 °C for 4 h. EDX spectroscopic analysis results are also given in (a).

prepared from Zn-Ga LDH and urea (R = 3) by calcination at 800 °C for 4 h. Comparison of this image with the SEM image of Zn-Ga LDH in Figure 1b clearly revealed that the hexagonal shape of Zn-Ga LDH was destroyed and the sample consisted primarily of well-crystallized particles with diameters of ca. 20–50 nm. It is noteworthy that nanocrystalline GaN:ZnO was obtained from the LDH precursor with a diameter of micrometer scale. As mentioned above, a large amount of Zn (ca. 50%) is lost during the nitridation process. Such volatilization of Zn likely leads to the decomposition of huge platelets of the precursor into the nanocrystalline nature of products. EDX spectroscopic analysis was carried out for several spot areas. The results revealed that there was almost no deviation in the atomic composition of the material from spot to spot, even in different primary particles. Previously, Maeda and co-workers reported that GaN:ZnO prepared by nitridation of Ga_2O_3 and ZnO using NH_3 gas possessed a nonuniform atomic composition even in the same primary particle.[24] In such a case, simultaneous diffusion of constituent ions of the starting mixture and nitridation occurred at the solid–solid boundary between Ga_2O_3 and ZnO. In contrast,

DOI: 10.1021/acs.inorgchem.8b02498
Inorg. Chem. XXXX, XXX, XXX–XXX

the constituent cations, i.e., Ga^{3+} and Zn^{2+}, were homogeneously mixed in the liquid-phase preparation process of Zn-Ga LDH. Although the authors of previous reports mentioned that the use of Zn-Ga LDH provided products with a uniform arrangement of Zn and Ga, no direct evidence for the uniform atomic composition of the same primary particle was given.[37−40] Our results suggest that Zn-Ga LDH is able to provide GaN:ZnO with highly uniform atomic composition. The bulk atomic composition of GaN:ZnO calcined at different temperatures was investigated by ICP-OES and is summarized in Table 1.[49] The Ga/Zn ratio in GaN:ZnO

Table 1. Relative Atomic Contents of Ga and Zn in GaN:ZnO Prepared from Zn-Ga LDH and Urea (R = 3) by Calcination at 800 °C for Various Periods

calcination duration/h	Ga	Zn
2	0.480	0.520
4	0.514	0.486
8	0.537	0.463
10	0.554	0.446

prepared by calcination for 4 h is close to 1. This result is in good correspondence to the result of EDX analysis. The Zn concentration tended to decrease with increasing calcination temperature, in good agreement with the XRD results. As mentioned in the previous section, volatilization of Zn induced by the high temperature during calcination decreased the Zn concentration of GaN:ZnO. Even after calcination for 10 h, the atomic ratio of Zn was 44.6%. Usually, GaN:ZnO prepared by the traditional method using a mixture of oxides as a precursor has a low Zn content (<30−40%). The use of Zn-Ga LDH enabled formation of Zn-rich GaN:ZnO. These results agreed well with those of previous papers for the preparation of GaN:ZnO using Zn-Ga LDH.[37−40] A UV−vis diffuse reflectance spectrum for GaN:ZnO prepared from Zn-Ga LDH and urea (R = 3) by calcination at 800 °C for 4 h is shown in Figure 5b. Consistent with optical photographs (Figure 2), the absorption edge of GaN:ZnO was at 530.2 nm, which is at longer wavelength than those of GaN and ZnO. The band gap (E_g) of the obtained GaN:ZnO was roughly estimated to be 2.34 eV, which was smaller than that of GaN:ZnO prepared by the conventional process using Ga_2O_3 and ZnO[24,28] and corresponded to that of previously reported GaN:ZnO prepared from Zn-Ga LDH and nitrided using gaseous NH_3.[37−39] These results suggest that GaN:ZnO prepared from Zn-Ga LDH and urea is of high quality, comparable with that prepared by the conventional procedure using Ga_2O_3, ZnO, and NH_3 gas. The absorption edge and E_g values of GaN:ZnO prepared by calcination at 900 °C for 4 h are 451.7 nm and 2.75 eV, respectively (Figure S8). The blue shift of the absorption edge, i.e. the increase in the E_g value, is consistent with the decrease in Zn content in GaN:ZnO by the volatilization. These results suggest that the band gap of GaN:ZnO prepared from Zn-Ga LDH and urea can be tuned by the calcination temperature.

Nitridation Mechanism of Zn-Ga LDH To Form GaN:ZnO. Previously, several research groups reported the preparation of metal oxynitrides, such as TaON and $LaTiO_2N$, using urea as a nitriding agent.[44,46] Thermal decomposition of urea in the absence of H_2O can be written as[50]

$$H_2NCONH_2 \rightarrow NH_3 + HCNO\ (140\ ^\circ C) \quad (2)$$

$$H_2NCONH_2 \rightarrow H_2O + H_2CN_2\ (140\ ^\circ C) \quad (3)$$

Gomathi and co-workers argued that NH_3 generated by decomposition of urea can react with metal carbonates and transition metal oxides to yield metal oxynitrides.[44] Conversely, in the typical synthesis of GaN:ZnO by ammonolysis, the nitridation of metal oxides usually occurs at relatively high temperatures (e.g. 800 °C).[20−24] Judging from the heating rate, the NH_3 generated by decomposition of urea should flow away from the reaction tube before reaching the reaction temperature (>600 °C) in the current system because the reaction was carried out under a N_2 stream. Therefore, to determine the behavior of the urea-decomposed species, we performed heat treatment at lower temperatures. Figure 6 shows XRD patterns

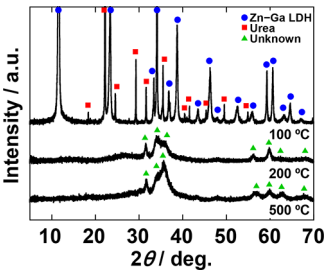

Figure 6. XRD patterns of products obtained from mixtures of Zn-Ga LDH and urea after heat treatment at 100, 200, and 500 °C for 4 h.

of the products obtained from mixtures of Zn-Ga LDH and urea after heat treatment at 100, 200, and 500 °C. For the mixture heated at 100 °C, diffraction peaks indexed to Zn-Ga LDH and urea were observed in the XRD pattern and no other peaks were found. This suggests that no decomposition of LDH or urea occurred at 100 °C. In contrast, these peaks completely disappeared and unknown peaks were found for the sample heated above 200 °C. This result indicates that Zn-Ga LDH and urea decomposed between 100 and 200 °C, corresponding to the decomposition temperature of urea (140 °C). Unknown peaks were observed in the pattern of the samples heated at 200 and 500 °C. Therefore, intermediate compounds are believed to form in this temperature region. We predict that these "unknown" intermediate species play important roles in the nitridation of Zn-Ga LDH to form GaN:ZnO.

XAFS is an excellent method to investigate the local bonding and short-range order of complex systems such as GaN:ZnO because it can afford very high sensitivity and elemental specificity.[51] Therefore, we tried to identify the intermediate species found in the XRD patterns in Figure 6 using XAFS measurements. First, Ga and Zn K-edge XANES studies were carried out. Ex situ Ga and Zn K-edge XANES spectra of mixtures of Zn-Ga LDH and urea heat treated at 100, 200, 300, 400, 500, 600, 700, and 800 °C are given in Figure 7b,d. In addition, XANES spectra of reference standards, i.e., Zn-Ga LDH, ZnO, Ga_2O_3, GaN, $Zn(CN_2)$, and GaN:ZnO, were also measured (Figure 7a,c). The shapes of spectra for both Ga and Zn drastically changed after the heating temperature reached 200 °C, indicating the collapse of the structure of LDH. In Ga K-edge XANES spectra, the contribution from the Ga-N local structure analogous to GaN or GaN:ZnO was not found at intermediate temperatures (200−600 °C). A contribution from Ga_2O_3 was observed when the heating temperature reached 200 °C (Figure 7b). The peaks assignable to

DOI: 10.1021/acs.inorgchem.8b02498
Inorg. Chem. XXXX, XXX, XXX−XXX

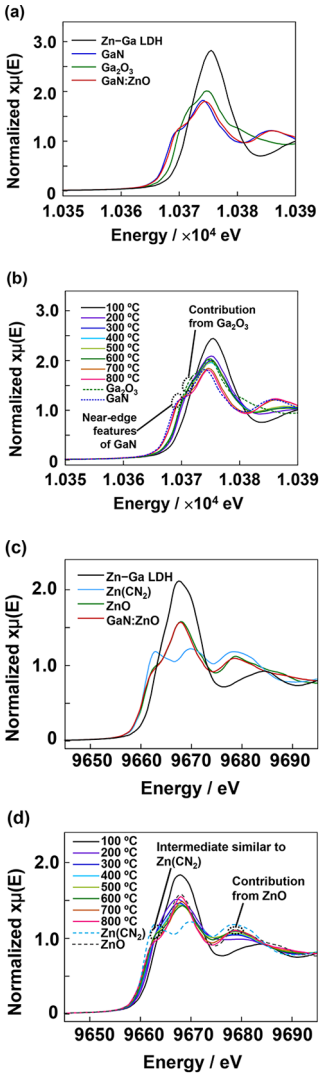

Figure 7. (a, b) Ga K-edge and (c, d) Zn K-edge ex situ XANES spectra of samples. Spectra of standard samples (Zn-Ga LDH, GaN, Ga_2O_3, $Zn(CN_2)$, ZnO, and GaN:ZnO) are given in (a) and (c). Spectra of mixtures of Zn-Ga LDH and urea heat treated at 100, 200, 300, 400, 500, 600, 700, and 800 °C are given in (b) and (d).

crystalline Ga_2O_3 were not found in the XRD patterns of the sample prepared at these temperature ranges (Figure 6). Therefore, though the intermediate species have local structure corresponding to Ga_2O_3, it cannot be detected by XRD because it was not well crystallized or was in the amorphous state. This contribution disappeared in the spectra for the samples heat treated above 600 °C. The spectrum for the sample treated at 700 °C exhibited near edge features consistent with those of GaN. These results suggest that Ga components are not directly nitrided by NH_3 generated via the decomposition of urea. In Zn K-edge XANES spectra of the samples treated above 200 °C, the shape of the spectra indicates the formation of intermediate states containing chemical environments similar to that of $Zn(CN_2)$ (Figure 7d). A contribution from ZnO was identified when the heating temperature reached 500 °C and remained in the spectrum of the sample treated at 600 °C. The Zn K-edge XANES spectrum of the sample heat treated at 800 °C agreed well with that of GaN:ZnO. Thus, the XAFS measurements confirm the optimal synthesis temperature of GaN:ZnO derived from XRD measurements (800 °C).

We also carried out in situ Ga and Zn K-edge XANES studies (Figure S9). The in situ XANES measurements were conducted using pellets composed of mixtures of Zn-Ga LDH, urea, and diluent heat treated at temperatures from 100 to 800 °C. The variation of in situ XANES spectra almost corresponded to that of the ex situ spectra. Therefore, the ex-situ XANES results reflect well the nitridation process from Zn-Ga LDH to GaN:ZnO. To examine the contributions of chemical species to the Ga and Zn K-edge XANES spectra during heat treatment of the mixtures of Zn-Ga LDH and urea, we fitted the absorption coefficients with linear combinations of Zn-Ga LDH, Ga_2O_3, and GaN:ZnO for Ga and Zn-Ga LDH, $Zn(CN_2)$, and GaN:ZnO for Zn (Figure S10). The results suggest that the sample in the intermediate state during heat treatment in the region from 200 to 600 °C contained chemical species with a local structure similar to that of $Zn(CN_2)$.

Ga and Zn K-edge ex situ EXAFS spectra of mixtures of Zn-Ga LDH and urea heat treated at 100, 200, 600, and 700 °C are displayed in Figure 8. Here we focused on the first coordination shell region. The Ga and Zn K-edge ex situ EXAFS spectra for standard materials, i.e., Zn-Ga LDH, ZnO, Ga_2O_3, GaN, $Zn(CN_2)$, and GaN:ZnO, were also examined. In the sample heat treated at 100 °C, both Ga and Zn existed in Ga−O and Zn−O coordination environments of Zn-Ga LDH, respectively. Consistent with the XRD and XANES results, the peaks assignable to Zn-Ga LDH remained in the EXAFS spectrum of the sample heat treated at 100 °C. The peak positions of both Ga and Zn were shifted markedly to shorter distances when the heat treatment temperature was raised to 200 °C. The XRD results revealed that the LDH structure collapsed when the samples were heat treated above 200 °C. In the Ga K-edge EXAFS spectra, the peak appeared at the position corresponding to the Ga−O coordination environment of Ga_2O_3. When the heat treatment was carried out at 600 °C, the peak was still found at the same position (Figure 8b). Conversely, the peak shifted to longer distance corresponding to the generation of the Ga−N coordination environment of GaN:ZnO for the sample heat treated at 700 °C. These results indicate that Ga−N bonds were generated in the high-temperature region (>700 °C) during the heat treatment process. These results also suggest that NH_3 generated at ca. 140 °C does not directly induce nitridation of Zn-Ga LDH to GaN:ZnO. In the Zn K-edge EXAFS spectra, there is no distinct difference between the positions of the peaks from the Zn−O coordination environment of ZnO and those from the Zn−N coordination environment of $Zn(CN_2)$ (Figure 8d).

Formation of metal cyanamide species was also supported by FT-IR spectroscopy measurements, as shown in Figure 9. Diffuse-reflectance FT-IR spectra were obtained for mixtures of Zn-Ga LDH and urea heat treated at 100, 200, 500, 700, and 800 °C (Figure 9a). For reference, FT-IR spectra of Zn-Ga LDH, urea, and $Zn(CN_2)$ are also given in Figure 9b. Pristine $Zn(CN_2)$ displayed strong characteristic absorption bands around 1880−2170 cm^{-1} corresponding to the asymmetric stretching modes of $[NCN]^{2-}$.[52−55] These bands are consistent with previous reports of $Zn(CN_2)$ and also with the IR spectra of the cyanamides of cobalt, nickel, and manganese.[54,55] The FT-IR spectrum for the sample heat treated at 100 °C was similar to that for pristine Zn-Ga LDH

DOI: 10.1021/acs.inorgchem.8b02498
Inorg. Chem. XXXX, XXX, XXX−XXX

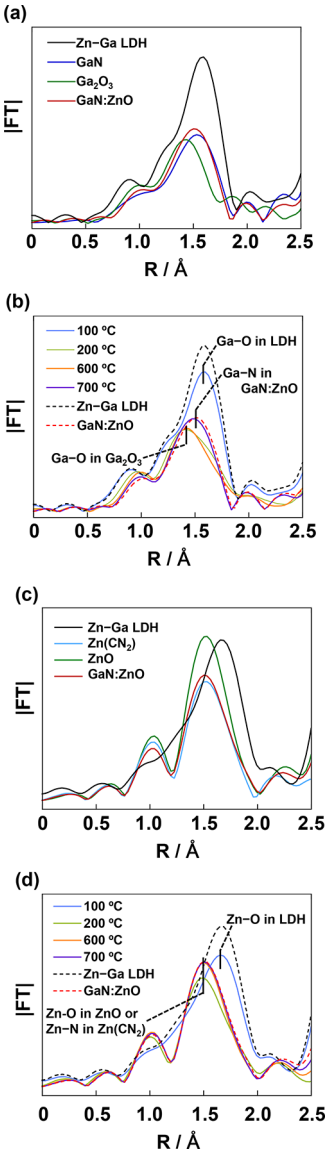

Figure 8. Fourier-transformed EXAFS spectra at (a, b) the Ga K-edge and (c, d) Zn K-edge. Spectra of standard samples (Zn-Ga LDH, GaN, Ga_2O_3, $Zn(CN_2)$, ZnO, and GaN:ZnO) are given in (a) and (c). Spectra of mixtures of Zn-Ga LDH and urea heat treated at 100, 200, 600, and 700 °C are given in (b) and (d).

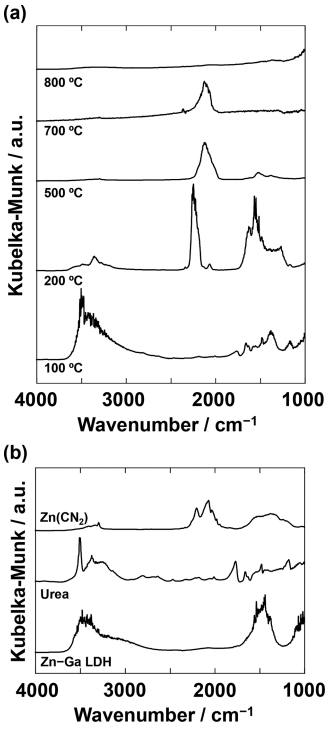

Figure 9. FT-IR spectra of (a) mixtures of Zn-Ga LDH and urea heat treated at 100, 200, 500, 700, and 800 °C and (b) standard samples (Zn-Ga LDH, urea, and $Zn(CN_2)$).

The obtained Q-MS curves are presented in Figure 10. During heating of a mixture of Zn-Ga LDH and urea, CO_2 (m/z 44),

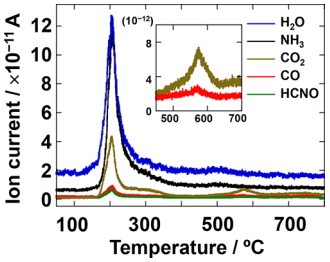

Figure 10. Q-MS analysis of gas evolution during heat treatment of a mixture of Zn-Ga LDH and urea. The inset shows magnified data for CO_2 and CO from 450 to 700 °C.

and did not contain any peaks around 2000 cm^{-1}. In contrast, strong absorption bands assignable to $[NCN]^{2-}$ were found in the spectrum for the sample heat treated at 200 °C. These bands also existed in the spectra for the samples heat treated at 500 and 700 °C. Therefore, C and N components in urea are converted to $[NCN]^{2-}$ species after decomposition around 150 °C and these $Zn(CN_2)$-like species exist as intermediates during heat treatment. The characteristic absorption bands of $[NCN]^{2-}$ completely disappeared in the spectrum for the sample heat treated at 800 °C. This suggests that the intermediate cyanamide species decomposed at high temperature (700−800 °C) to give the oxynitride solid solution: i.e., GaN:ZnO. These results agreed well with those of XRD and XAFS measurements.

To further investigate the nitridation process using urea, the evolved gas was analyzed by Q-MS. This technique detects the gases released during heat treatment using He as a carrier gas. H_2O (m/z 18), NH_3 (m/z 17), and HCNO (m/z 43) were generated in the temperature range from 130 to 250 °C. As shown in Figure 6, crystalline phases of Zn-Ga LDH and urea disappeared after heating at 200 °C. In addition, it has been reported that the decomposition of urea occurs at 140 °C, as shown in eq 2. Therefore, this result coincides with the decomposition of Zn-Ga LDH and urea. It is clear that the release of NH_3 gas caused by urea decomposition occurred until the temperature reached 300 °C. Therefore, direct nitridation of Zn-Ga LDH to form GaN:ZnO by NH_3 gas is impossible because NH_3 gas does not exist in the temperature region required for formation of oxynitrides: e.g., 850 °C. At temperatures above 600 °C, CO_2 (m/z 44) and CO (m/z 28) were released. The peak at m/z 28 could also correspond to N_2; however, the presence of a fragment with m/z 12 corresponding to C and absence of a fragment with m/z 14 corresponding to N confirmed that the peak at m/z 28

DOI: 10.1021/acs.inorgchem.8b02498
Inorg. Chem. XXXX, XXX, XXX−XXX

originated from CO rather than N_2. Before this temperature range was reached, the release of CO_2 from interlayer CO_3^{2-} via decomposition of Zn-Ga LDH was already complete. This suggests that the origin of CO_2 and CO is decomposition of $Zn(CN_2)$-like species, which were detected in the FT-IR spectra.

Considering the results of XRD, XAFS, FT-IR, and Q-MS analyses, we propose a nitridation mechanism of Zn-Ga LDH to form GaN:ZnO using urea as a nitrogen source, which is shown in Scheme 1. First, Zn-Ga LDH and urea decompose around 150 °C and release CO_2, H_2O, and NH_3 gases. Then, the Zn component in LDH forms the $Zn(CN_2)$-like species by reaction with HCNO and/or H_2CN_2 generated by urea decomposition. The Ga component in LDH also forms the Ga_2O_3-like intermediate at this stage. When the temperature reaches 600 °C, decomposition of the $Zn(CN_2)$-like species occurs through reaction with the Ga_2O_3-like intermediate. At this stage, generation of Ga−N bonds and release of CO_2 and CO gases started. Finally, crystallization of the solid solution of GaN:ZnO in a wurtzite phase was completed at 800 °C.

Scheme 1. Schematic Outlining the Formation Mechanism of GaN:ZnO using Zn-Ga LDH and Urea as a Precursor and a Nitriding Agent, Respectively

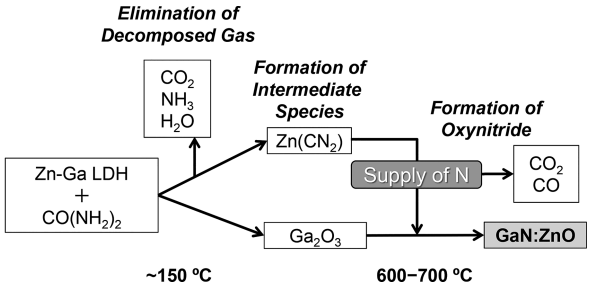

CONCLUSIONS

A new method for the facile preparation of GaN:ZnO solid solutions was developed. The use of Zn-Ga LDH as a precursor provided uniform atomic distributions of Zn and Ga in GaN:ZnO. In addition, urea was used as a safe solid-state nitriding agent, avoiding the need for corrosive NH_3. By the optimization of reaction conditions such as heat treatment temperature and ratio of urea, single-phase GaN:ZnO was successfully obtained. A lower heat treatment temperature and higher ratio of urea gave $Zn(CN_2)$ as a byproduct. Conversely, $ZnGa_2O_4$ formed as a byproduct when the ratio of urea was low or heat treatment was carried out for more than 12 h. We carefully analyzed the nitridation mechanism. First, Zn-Ga LDH and urea decomposed to generate $Zn(CN_2)$- and Ga_2O_3-like species as intermediates at ca. 150 °C. Second, the $Zn(CN_2)$-like species decomposed and Ga−N bond generation started around 600 °C. Finally, the crystallization of the solid solution of GaN:ZnO in a wurtzite phase was completed at 800 °C. We revealed that the formation of $Zn(CN_2)$-like species played an important role during the nitridation process and NH_3 gas released from the decomposition of urea did not act as a nitriding agent in this system. Because of the safety, low cost, and simplicity of this process, we believe that nitridation using urea will open up opportunities for the facile synthesis of various metal oxynitrides. In addition, the characterization strategy used in this work, i.e. ex situ and in situ XAFS, FT-IR, and Q-MS measurements, should be extremely effective to analyze the formation process of oxynitrides using urea as a nitriding agent. Therefore, the preparation of various kinds of oxynitrides and investigation of the nitridation mechanism are currently being performed by our research team.

ASSOCIATED CONTENT

Supporting Information

The Supporting Information is available free of charge on the ACS Publications website at DOI: 10.1021/acs.inorgchem.8b02498.

Preparation of standard samples of $ZnGa_2O_4$ and $Zn(CN_2)$ for XAFS measurements, XRD patterns of $ZnGa_2O_4$ and $Zn(CN_2)$, shifts of the (101) diffraction peak of GaN:ZnO, optical photograph of GaN:ZnO samples prepared at various temperatures and for different durations, XRD pattern of the sample prepared using a mixture of Ga_2O_3 and ZnO as a precursor instead of Zn-Ga LDH, in situ XANES spectra, and linear combination fitting XANES analysis (PDF)

AUTHOR INFORMATION

Corresponding Author

*E-mail for K.K.: kktgr@hiroshima-u.ac.jp.

ORCID

Kiyofumi Katagiri: 0000-0002-9548-9835
Kei Inumaru: 0000-0001-6876-3854
Kazuhiko Maeda: 0000-0001-7245-8318

Author Contributions

The manuscript was written through contributions of all authors. All authors have given approval to the final version of the manuscript.

Notes

The authors declare no competing financial interest.

ACKNOWLEDGMENTS

This work was supported by JSPS KAKENHI Grant Nos. JP16H06438, JP16H06441, JP17H05483, and JP17H03392. This work was partially supported by the Center for Functional Nano Oxide at Hiroshima University. The synchrotron radiation experiments were performed at the BL01B1 beamline of SPring-8 with the approval of the Japan Synchrotron Radiation Research Institute (JASRI) (Proposal Nos. 2017B1043 and 2018A1749). We thank Natasha Lundin, Ph.D., from the Edanz Group (www.edanzediting.com/ac) for editing a draft of this manuscript.

REFERENCES

(1) Lewis, N. S.; Nocera, D. G. Powering the Planet: Chemical Challenges in Solar Energy Utilization. *Proc. Natl. Acad. Sci. U. S. A.* **2006**, *103*, 15729−15735.
(2) Kamat, P. V. Meeting the Clean Energy Demand: Nanostructure Architectures for Solar Energy Conversion. *J. Phys. Chem. C* **2007**, *111*, 2834−2860.
(3) Schlögl, R. The Role of Chemistry in the Energy Challenge. *ChemSusChem* **2010**, *3*, 209−222.
(4) Kudo, A.; Miseki, Y. Heterogeneous Photocatalyst Materials for Water Splitting. *Chem. Soc. Rev.* **2009**, *38*, 253−278.
(5) Walter, M. G.; Warren, E. L.; McKone, J. R.; Boettcher, S. W.; Mi, Q.; Santori, E. A.; Lewis, N. S. Solar Water Splitting Cells. *Chem. Rev.* **2010**, *110*, 6446−6473.

DOI: 10.1021/acs.inorgchem.8b02498
Inorg. Chem. XXXX, XXX, XXX−XXX

(6) Maeda, K.; Domen, K. Photocatalytic Water Splitting: Recent Progress and Future Challenges. *J. Phys. Chem. Lett.* **2010**, *1*, 2655−2661.
(7) Hisatomi, T.; Kubota, J.; Domen, K. Recent Advances in Semiconductors for Photocatalytic and Photoelectrochemical Water Splitting. *Chem. Soc. Rev.* **2014**, *43*, 7520−7535.
(8) Li, X.; Yu, J.; Low, J.; Fang, Y.; Xiao, J.; Chen, X. Engineering Heterogeneous Semiconductors for Solar Water Splitting. *J. Mater. Chem. A* **2015**, *3*, 2485−2534.
(9) Fujishima, A.; Zhang, X.; Tryk, D. A. TiO_2 Photocatalysis and Related Surface Phenomena. *Surf. Sci. Rep.* **2008**, *63*, 515−582.
(10) Taştan, Ü.; Ziegenbalg, D. Getting the Most Out of Solar Irradiation: Efficient Use of Polychromatic Light for Water Splitting. *Chem. - Eur. J.* **2016**, *22*, 18824−18832.
(11) Youngblood, W. J.; Lee, S.-H. A.; Maeda, K.; Mallouk, T. E. Visible Light Water Splitting Using Dye-Sensitized Oxide Semiconductors. *Acc. Chem. Res.* **2009**, *42*, 1966−1973.
(12) Maeda, K.; Domen, K. Development of Novel Photocatalyst and Cocatalyst Materials for Water Splitting under Visible Light. *Bull. Chem. Soc. Jpn.* **2016**, *89*, 627−648.
(13) Chen, J.; Wu, X.-J.; Yin, L.; Li, B.; Hong, X.; Fan, Z.; Chen, B.; Xue, C.; Zhang, H. One-Pot Synthesis of CdS Nanocrystals Hybridized with Single-Layer Transition-Metal Dichalcogenide Nanosheets for Efficient Photocatalytic Hydrogen Evolution. *Angew. Chem., Int. Ed.* **2015**, *54*, 1210−1214.
(14) Williams, R. Becquerel Photovoltaic Effect in Binary Compounds. *J. Chem. Phys.* **1960**, *32*, 1505−1514.
(15) Ellis, A. B.; Kaiser, S. W.; Bolts, J. M.; Wrighton, M. S. Study of n-Type Semiconducting Cadmium Chalcogenide-Based Photoelectrochemical Cells Employing Polychalcogenide Electrolytes. *J. Am. Chem. Soc.* **1977**, *99*, 2839−2848.
(16) Moriya, Y.; Takata, T.; Domen, K. Recent Progress in the Development of (Oxy)nitride Photocatalysts for Water Splitting under Visible-Light Irradiation. *Coord. Chem. Rev.* **2013**, *257*, 1957−1969.
(17) Fuertes, A. Metal Oxynitrides as Emerging Materials with Photocatalytic and Electronic Properties. *Mater. Horiz.* **2015**, *2*, 453−461.
(18) Takata, T.; Domen, K. Development of Non-Oxide Semiconductors as Light Harvesting Materials in Photocatalytic and Photoelectrochemical Water Splitting. *Dalton Trans.* **2017**, *46*, 10529−10544.
(19) Abeysinghe, D.; Skrabalak, S. E. Toward Shape-Controlled Metal Oxynitride and Nitride Particles for Solar Energy Applications. *ACS Energy Lett.* **2018**, *3*, 1331−1344.
(20) Maeda, K.; Takata, T.; Hara, M.; Saito, N.; Inoue, Y.; Kobayashi, H.; Domen, K. GaN:ZnO Solid Solution as a Photocatalyst for Visible-Light-Driven Overall Water Splitting. *J. Am. Chem. Soc.* **2005**, *127*, 8286−8287.
(21) Maeda, K.; Teramura, K.; Takata, T.; Hara, M.; Saito, N.; Toda, K.; Inoue, Y.; Kobayashi, H.; Domen, K. Overall Water Splitting on $(Ga_{1-x}Zn_x)(N_{1-x}O_x)$ Solid Solution Photocatalyst: Relationship between Physical Properties and Photocatalytic Activity. *J. Phys. Chem. B* **2005**, *109*, 20504−20510.
(22) Maeda, K.; Teramura, K.; Lu, D.; Takata, T.; Saito, N.; Inoue, Y.; Domen, K. Photocatalyst Releasing Hydrogen from Water. *Nature* **2006**, *440*, 295.
(23) Maeda, K.; Teramura, K.; Masuda, H.; Takata, T.; Saito, N.; Inoue, Y.; Domen, K. Efficient Overall Water Splitting under Visible-Light Irradiation on $(Ga_{1-x}Zn_x)(N_{1-x}O_x)$ Dispersed with Rh−Cr Mixed-Oxide Nanoparticles: Effect of Reaction Conditions on Photocatalytic Activity. *J. Phys. Chem. B* **2006**, *110*, 13107−13112.
(24) Maeda, K.; Domen, K. Solid Solution of GaN and ZnO as a Stable Photocatalyst for Overall Water Splitting under Visible Light. *Chem. Mater.* **2010**, *22*, 612−623.
(25) Grabke, H. J. A Case of Nitridation, Carburization and Oxidation on a Stainless Steel. *Mater. Corros.* **2005**, *56*, 384−388.
(26) Hara, M.; Hitoki, G.; Takata, T.; Kondo, J. N.; Kobayashi, H.; Domen, K. TaON and Ta_3N_5 as New Visible Light Driven Photocatalysts. *Catal. Today* **2003**, *78*, 555−560.
(27) Lee, K.; Tienes, B. M.; Wilker, M. B.; Schnitzenbaumer, K. J.; Dukovic, G. $(Ga_{1-x}Zn_x)(N_{1-x}O_x)$ Nanocrystals: Visible Absorbers with Tunable Composition and Absorption Spectra. *Nano Lett.* **2012**, *12*, 3268−3272.
(28) Tongying, P.; Lu, Y.-G.; Hall, L. M. G.; Lee, K.; Sulima, M.; Ciston, J.; Dukovic, G. Control of Elemental Distribution in the Nanoscale Solid-State Reaction That Produces $(Ga_{1-x}Zn_x)(N_{1-x}O_x)$ Nanocrystals. *ACS Nano* **2017**, *11*, 8401−8412.
(29) Khan, A. I.; O'Hare, D. Intercalation Chemistry of Layered Double Hydroxides: Recent Developments and Applications. *J. Mater. Chem.* **2002**, *12*, 3191−3198.
(30) Wang, Q.; O'Hare, D. Recent Advances in the Synthesis and Application of Layered Double Hydroxide (LDH) Nanosheets. *Chem. Rev.* **2012**, *112*, 4124−4155.
(31) Fan, G.; Li, F.; Evans, D. G.; Duan, X. Catalytic Applications of Layered Double Hydroxides: Recent Advances and Perspectives. *Chem. Soc. Rev.* **2014**, *43*, 7040−7066.
(32) Mohapatra, L.; Parida, K. A Review on the Recent Progress, Challenges and Perspective of Layered Double Hydroxides as Promising Photocatalysts. *J. Mater. Chem. A* **2016**, *4*, 10744−10766.
(33) Fuda, K.; Kudo, N.; Kawai, S.; Matsuanga, T. Preparation of Zn/Ga-layered Double Hydroxide and Its Thermal Decomposition Behavior. *Chem. Lett.* **1993**, *22*, 777−780.
(34) Thomas, G. S.; Kamath, P. V. The Layered Double Hydroxide (LDH) of Zn with Ga: Synthesis and Reversible Thermal Behaviour. *Solid State Sci.* **2006**, *8*, 1181−1186.
(35) Zou, L.; Xiang, X.; Wei, M.; Li, F.; Evans, D. G. Single-Crystalline $ZnGa_2O_4$ Spinel Phosphor via a Single-Source Inorganic Precursor Route. *Inorg. Chem.* **2008**, *47*, 1361−1369.
(36) Valente, J. S.; López-Salinas, E.; Prince, J.; González, I.; Acevedo-Peña, P.; del Angel, P. Synthesis and Morphological Modification of Semiconducting Mg(Zn)Al(Ga)−LDH/ITO Thin Films. *Mater. Chem. Phys.* **2014**, *147*, 339−348.
(37) Wang, J.; Huang, B.; Wang, Z.; Wang, P.; Cheng, H.; Zheng, Z.; Qin, X.; Zhang, X.; Dai, Y.; Whangbo, M.-H. Facile Synthesis of Zn-rich $(GaN)_{1-x}(ZnO)_x$ Solid Solutions Using Layered Double Hydroxides as Precursors. *J. Mater. Chem.* **2011**, *21*, 4562−4567.
(38) Wang, J.; Yang, P.; Wang, Z.; Huang, B.; Dai, Y. Effect of Temperature on the Transformation from Zn-Ga Layered Double Hydroxides into $(GaN)_{1-x}(ZnO)_x$ Solid Solution. *J. Alloys Compd.* **2015**, *652*, 205−212.
(39) Chen, D. P.; Skrabalak, S. E. Synthesis of $(Ga_{1-x}Zn_x)(N_{1-x}O_x)$ with Enhanced Visible-Light Absorption and Reduced Defects by Suppressing Zn Volatilization. *Inorg. Chem.* **2016**, *55*, 3822−3828.
(40) Adeli, B.; Taghipour, F. Facile Synthesis of Highly Efficient Nano-Structured Gallium Zinc Oxynitride Solid Solution Photocatalyst for Visible-Light Overall Water Splitting. *Appl. Catal., A* **2016**, *521*, 250−258.
(41) Hu, Y.-L.; Ou, S.; Huang, J.; Ji, H.; Xiang, S.; Zhu, Y.; Chen, Z.; Gong, C.; Sun, L.; Lian, J.; Sun, D.; Fu, Y.; Ma, T. ZnGaNO Photocatalyst Particles Prepared from Methane-Based Nitridation Using Zn/Ga/CO_3 LDH as Precursor. *Inorg. Chem.* **2018**, *57*, 9412−9424.
(42) Knol, K. E.; Bramer, E. A.; Valk, M. Reduction of Nitrogen Oxides by Injection of Urea in the Freeboard of a Pilot Scale Fluidized Bed Combustor. *Fuel* **1989**, *68*, 1565−1569.
(43) Liu, M.; Wang, Y.; Wu, Y.; He, Z.; Wan, H. Greener" Adhesives Composed of Urea-Formaldehyde Resin and Cottonseed Meal for Wood-Based Composites. *J. Cleaner Prod.* **2018**, *187*, 361−371.
(44) Gomathi, A.; Reshma, S.; Rao, C. N. R. A Simple Urea-Based Route to Ternary Metal Oxynitride Nanoparticles. *J. Solid State Chem.* **2009**, *182*, 72−82.
(45) Giordano, C.; Erpen, C.; Yao, W.; Milke, B.; Antonietti, M. Metal Nitride and Metal Carbide Nanoparticles by a Soft Urea Pathway. *Chem. Mater.* **2009**, *21*, 5136−5144.

DOI: 10.1021/acs.inorgchem.8b02498
Inorg. Chem. XXXX, XXX, XXX−XXX

(46) Gao, Q.; Giordano, C.; Antonietti, M. Controlled Synthesis of Tantalum Oxynitride and Nitride Nanoparticles. *Small* **2011**, *7*, 3334−3340.
(47) Ravel, B.; Newville, M. *ATHENA, ARTEMIS, HEPHAESTUS*: Data Analysis for X-ray Absorption Spectroscopy Using IFEFFIT. *J. Synchrotron Radiat.* **2005**, *12*, 537−541.
(48) Shannon, R. D. Revised Effective Ionic Radii and Systematic Studies of Interatomic Distances in Halides and Chalcogenides. *Acta Crystallogr., Sect. A: Cryst. Phys., Diffr., Theor. Gen. Crystallogr.* **1976**, *32*, 751−767.
(49) Previous elemental analyses confirmed that the Ga/N and Zn/O ratios are close to 1 and that the N/O ratio increases with the Ga/Zn ratio.[20]
(50) Podsiadło, S. Stages of the Synthesis of Gallium Nitride with the Use of Urea. *Thermochim. Acta* **1995**, *256*, 367−373.
(51) Rehr, J. J.; Albers, R. C. Theoretical Approaches to X-Ray Absorption Fine Structure. *Rev. Mod. Phys.* **2000**, *72*, 621−654.
(52) Kaye, K. M.; Grantham, W.; Hyett, G. A Facile Route to Thin Films of Zinc Carbodiimide Using Aerosol-assisted CVD. *Chem. Vap. Deposition* **2015**, *21*, 281−287.
(53) Liu, X.; Müller, P.; Dronskowski, R. Synthesis and Crystal Structure of Ammine Copper(I) Cyanamide, $Cu_4(NCN)_2NH_3$. *Z. Anorg. Allg. Chem.* **2005**, *631*, 1071−1074.
(54) Liu, X.; Krott, M.; Müller, P.; Hu, C.; Lueken, H.; Dronskowski, R. Synthesis, Crystal Structure, and Properties of MnNCN, the First Carbodiimide of a Magnetic Transition Metal. *Inorg. Chem.* **2005**, *44*, 3001−3003.
(55) Krott, M.; Liu, X.; Fokwa, B. P. T.; Speldrich, M.; Lueken, H.; Dronskowski, R. Synthesis, Crystal-Structure Determination and Magnetic Properties of Two New Transition-Metal Carbodiimides: CoNCN and NiNCN. *Inorg. Chem.* **2007**, *46*, 2204−2207.

DOI: 10.1021/acs.inorgchem.8b02498
Inorg. Chem. XXXX, XXX, XXX−XXX